Journal of
Water & Climate Change

IWA PUBLISHING

Journal of Water and Climate Change Vol 14 No 7, 2432 doi: 10.2166/wcc.2023.114

Characteristics and attribution analysis of runoff and sediment evolution in the Wei River mainstream, China

Wenxian Guo, Ye Sang *, Jianwen Hu, Wenping Wang and Hongxiang Wang

North China University of Water Resources and Electric Power, Zhengzhou 450045, China
*Corresponding author. E-mail: 1343539712@qq.com

YS, 0009-0003-3628-0673

ABSTRACT

This study evaluates the characteristics of river runoff and sediment changes in the Wei River mainstream over the past 50 years based on runoff and sediment data and meteorological data from 1971 to 2020 at the Huaxian hydrological station in the lower reaches of the Wei River. The main research methods are the Mann–Kendall method, wavelet analysis, cross-wavelet analysis, and cumulative curve method. The results show that there is no significant decreasing trend and abrupt change in runoff volume in recent years, the decreasing trend of sediment transport is obvious, and the abrupt change occurs around 2006. The dominant periodicity of runoff is 12–13a, and the dominant periodicity of sediment transport is 5a. There is only a significant resonance periodicity of 3–5a in 1980–1990, which is roughly a positive correlation. The runoff–sediment series can be divided into four time periods, and the reasons for the change in the runoff–sediment relationship are different in each time period. The precipitation factor has a slightly greater impact on runoff and a weak impact on sediment transport, with contribution rates of 21.2 and 7.6%. Human activities such as subsurface changes and water conservancy construction have a greater impact on runoff and sediment load, with contribution rates of 78.8 and 92.4%.

Key words: climate change, cross-wavelet, human activities, land use, runoff–sediment relationship, Wei River

HIGHLIGHTS

- In this study, the resonance period between water and sediment is deeply studied by cross-wavelet analysis, and the mutual influence law between water and sediment in the mainstream of Weihe River is revealed.
- This study quantitatively assessed the impacts of climate change and human activities on runoff and sediment transport and analyzed the impact process in detail.

GRAPHICAL ABSTRACT

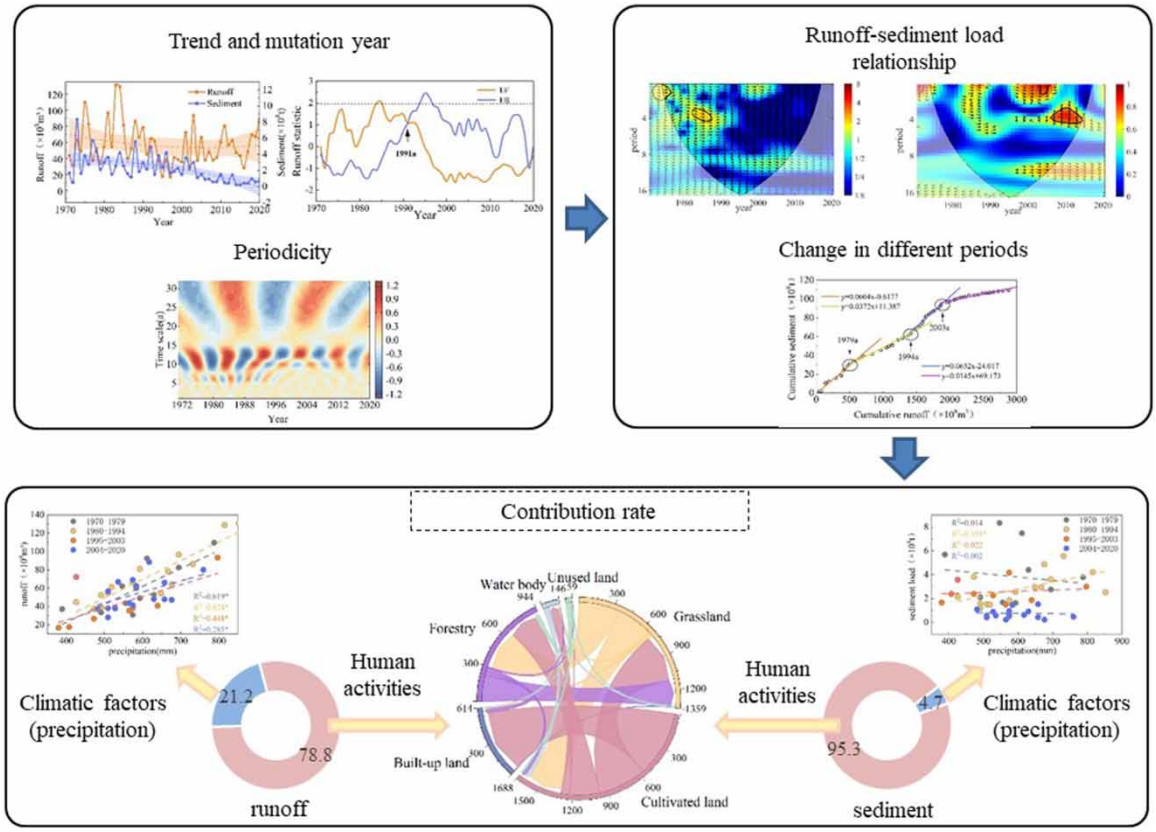

1. INTRODUCTION

River flooding and drought are common situations, and river management has been a great endeavor since ancient times in order to fight against nature (Song & Liu 2020; Brierley & Fryirs 2022). From simple containment in ancient times to concrete dams today, the impact of human activities on rivers has become increasingly prominent with the rapid development of society and technology (Liu *et al.* 2021a). Rivers evolve over a long period of time to develop unique regular characteristics, but due to strong disturbances from external factors, river conditions may change qualitatively at some point in time (Ye *et al.* 2020), such as runoff, sediment content, periodicity, and water quality conditions (Xu *et al.* 2011). According to statistics, the number of rivers with altered runoff worldwide is 24% of the total, and the number of rivers with altered sediment load is even higher, at around 40%. Few rivers in the world are in their natural state due to human disturbances (Li *et al.* 2020a). However, these river dynamics are important for understanding long-term water quality and ecological changes in the basin, so runoff and sediment changes have become an important topic of research (Mikhailov 2010; Li *et al.* 2020b).

Soil erosion is now one of the major environmental problems in the world, with the Yellow River basin bearing the brunt of the problem (Shi *et al.* 2010). The Loess Plateau in the basin has suffered serious ecological damage due to low vegetation cover and a high frequency of heavy rainfall coverage, and the sediment content in the river is high. These factors have caused serious sediment accumulation in the middle and lower reaches of the river, and the phenomenon of above-ground rivers is common, which seriously hinders the sustainable development of society (Schnitzer *et al.* 2013). In recent decades, human activities have greatly altered the underlying surface of the Loess Plateau, and the climate has changed significantly due to increased global warming from carbon dioxide, both of which have led to significant changes in the sedimentation of runoff from Loess Plateau rivers into the Yellow River (Tian *et al.* 2019). The Wei River is the first major tributary of the Yellow River, flowing through the Loess Plateau and converging in the middle reaches of the Yellow River, delivering 389 million tons of sediment and 7.45 billion m^3 of water to the Yellow River each year, accounting for approximately 39.87 and 26.03% of the total sediment and water volume of the Yellow River, making it a relatively

representative tributary (Chang *et al.* 2016). The Wei River is also an important source of water for humans in Shaanxi Province, supporting the operation of the grain-producing and industrial and commercial areas of the basin (Zhao *et al.* 2019). The study and analysis of runoff–sediment changes and their driving mechanisms in the changing environment of the Wei River basin (WRB) can help to analyze and predict the erosion and sediment production mechanisms and sediment load patterns in the Yellow River basin, which has important theoretical and practical significance for the prevention and control of soil erosion and also has significant strategic importance for the economic development of this basin (Deng *et al.* 2018; Zhang *et al.* 2022b).

The Wei River is located in the southeastern part of the Loess Plateau, which is an arid and semiarid region with a continental monsoon climate, so water resources are affected by the seasons. Droughts occur mainly in spring in the middle and upper reaches, are prone to occur in summer and autumn in the lower reaches, and occur mainly in winter in the tributaries, and there is a tendency for the severe development of droughts (Fan *et al.* 2022). Some studies have shown that this factor has a significant impact on runoff–sediment changes (Zhao *et al.* 2017). Secondly, the vegetation distribution in the watershed is discontinuous, and the ecological environment is fragile and extremely sensitive to human activities. People's excessive land reclamation and development have caused massive land erosion (Han *et al.* 2021; Zhang *et al.* 2022a). The sediment-producing areas are mainly located in the Jing and Beiluo River basins and the upper basin of the Wei River mainstream, where sediment accumulates in the lower reaches and is washed into the Yellow River, transporting large amounts of sediment to the Yellow River (Song *et al.* 2010). Huang *et al.* (2016) analyzed the contribution rate of climate and human activities to runoff reduction in different periods and found that human activities are the main driving factors of runoff reduction. Tian *et al.* (2022) analyzed the sediment load data of 15 hydrological stations in WRB and found that the sediment load in the basin decreased significantly, and rainfall, vegetation, and runoff all affected the sediment change. Most studies focus on the analysis of the variation trend and attribution of runoff and sediment load alone, but do not specifically study the internal relationship and correlation between runoff and sediment. This paper not only studies the interannual variation of runoff and sediment load in the mainstream of the Wei River but also studies the resonance cycle and interaction effect of runoff and sediment load based on cross-wavelet analysis and cumulative curve, and further expounds the relationship between sediment load and runoff. In addition, this paper also discusses in detail the impact of climate change and shadow activities on runoff and sediment changes, and emphatically analyzes the impact of terraced fields on sediment load, which provides more theoretical basis and ideas for ecological management.

2. STUDY AREA AND DATA

The mainstream of the Wei River is 818 km long, straddling eastern Gansu and central Shaanxi, and consists of the Gansu and Shaanxi sections, with a basin area of 106,498 km^2 (Wang *et al.* 2022). The upper section of the river is mostly gullies with peaks and valleys, while the lower section is flatter and more shallow (see Figure 1), with the Loess Hills and Gullies being the main area types (Jiang *et al.* 2015). The WRB has a warm semiarid continental monsoon climate with more rainfall in hot summers and less rainfall in cold winters and severe soil erosion (Shen & Qiang 2014). In this watershed, soil erosion affects an area of 84,200 km^2, or roughly 80% of the watershed, and the average annual sediment flow can be as high as 492 million tons (Wang *et al.* 2019).

Huaxian hydrological station, located in the lower reaches of the Wei River, is the control section where the Wei River flows into the Yellow River. It is more representative of runoff and sediment load and can well reflect the river state before the Wei River flows into the Yellow River. Therefore, the runoff and sediment load data from the Huaxian hydrological station from 1971a to 2020a were used to analyze the evolution of runoff and sediment in the Wei River and the interaction between the two, where the runoff data are measured runoff. Runoff and sediment load data for the Wei River Huaxian station from 1971a to 2020a were obtained from the *China River Sediment Bulletin*, and the precipitation data were obtained from the website of the China Meteorological Science Data Service Center (http://www.nmic.cn). Land use data come from the Resources and Environmental Science and Data Center of Chinese Academy of Sciences (http://www.resdc.cn).

3. METHODOLOGY

3.1. Mann–Kendall test

The Mann–Kendall (M–K) method is a common method for analyzing serial trends and testing for mutations. Let the time series data be X_1, X_2, …, X_n, and construct the test statistic Z after defining the statistic S. At a given significance level, if

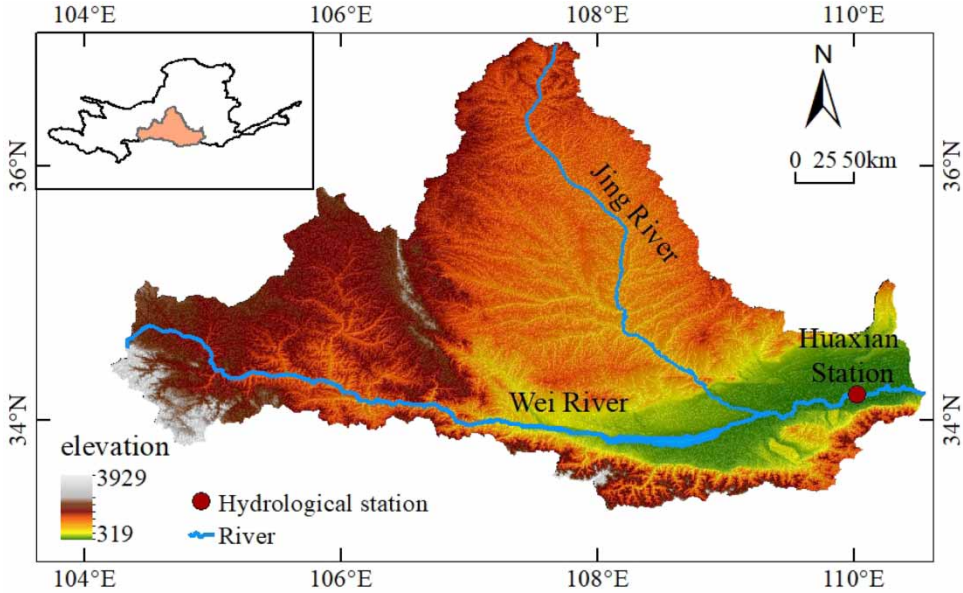

Figure 1 | Topography of the mainstream of the Wei River.

$|Z| > Z_{1-\alpha/2}$, the upward or downward trend of the series is significant at that significance level. When $Z > 0$, it indicates an upward trend, and vice versa, it indicates a downward trend.

The series of data was standardized according to the formula, and the calculated standard variation UF_k formed the UF curve. The UB_k and UB curves are obtained by the same method for its inverse series. The intersection of the curves UB and UF is the abrupt change points of the sequence. The specific methods and formulas for the calculation have been described in detail in other literature and will not be repeated here (Gocic & Trajkovic 2013; Ay & Kisi 2017). When $UF > 0$, it means that the sequence has an upward trend, and when $UF < 0$, the sequence has a downward trend.

3.2. Mean difference *t*-test

When multiple intersections occur in the series using the M–K method, a significance test is required to determine whether they are abrupt change points. In the mean difference *t*-test method, the series is divided into two time periods, before and after, with the intersection point as the dividing line, and if the mean difference between the two time periods exceeds the statistical significance, it is considered that a mutation occurs at the selected time point within a certain level of significance (Zhang 2010). The statistic T was defined as

$$T = (X_{1P} - X_{2P})/[S_P(1/M_1 + 1/M_2)^{0.5}] \quad (1)$$

$$S_p^2 = [(M_1 - 1)S_1^2 + (M_2 - 1)S_2^2]/(M_1 + M_2 - 2) \quad (2)$$

where M_1 and M_2 are the sample lengths of the two sequences before and after the mutation year, X_{1p} and X_{2p} are the means, S_1 and S_2 are the standard deviations, S_p is the joint sample variance. When a certain significant level α is given, if $t<t_\alpha$, there is a significant difference between the means on both sides of the mutation point at the significant level of α, i.e., there is an abrupt change at that point.

3.3. Wavelet analysis

Wavelet transform analysis is an effective tool to study the periodic and nonperiodic characteristics of nonstationary, multi-scale time series of hydrological processes. At this time, complex Morlet wavelets are used to analyze the WRB (Sang *et al.* 2016). The continuous wavelet function is as follows:

$$W_f(a, b) = |a|^{-1/2} \int_R f(t)\bar{\varphi}\left(\frac{t-b}{a}\right)dt \quad (a, b \in R, a \neq 0) \quad (3)$$

where $W_f(a,b)$ is the wavelet transform coefficient, $f(t)$ is the known signal, a is the scale factor, which represents the period length, b is the time translation length, $\bar{\varphi}\left(\frac{t-b}{a}\right)$ is the conjugate complex of $\varphi\left(\frac{t-b}{a}\right)$ (Guo *et al.* 2022).

3.4. Cross-wavelet transform

The wavelet transform is commonly used to analyze the regular transform of a time series, and cross-wavelets incorporate cross-spectral analysis on its basis to be able to analyze the correlation between two time series in the simultaneous domain (Durocher *et al.* 2016). Assuming that the two time series are $X(n)$ and $Y(n)$, the wavelet transform coefficients of the series can be found, denoted as $W_n^x(s)$, $W_n^y(s)$ and the cross-wavelet spectrum between the two series is written as

$$W_n^{xy}(s) = W_n^x(s) \times W_n^{y*}(s) \tag{4}$$

where $W_n^{y*}(s)$ is the complex conjugate of $W_n^y(s)$. The magnitude of the $|W_n^{xy}(s)|$ value is related to the degree of correlation between the two sequences: the larger the value, the higher the correlation, and vice versa, the lower the correlation. The principle of the above method has been described in detail and will not be repeated here (Ghaderpour *et al.* 2018).

3.5. Slope change ratio of accumulative quantity

The amount that climate change and human activity influence runoff and sediment flow can be quantified using the slope change approach. Precipitation is used as a representative factor of climate change because evapotranspiration has a small effect on runoff. Assuming that only one of the two factors affects runoff and sediment, the slope of the curve for runoff or sediment should change in proportion to that factor. If the multiplicity is different, however, it is likely that the other factor also has an impact. By defining the total degree of influence as 1, the contribution of human activities can be deduced by determining the percentage of influence of precipitation. If the cumulative slope before the change is Y_{Ra} and the cumulative slope after the change is Y_{Rb}, the rate of change of the cumulative runoff slope K_R (%) is

$$K_R = \frac{Y_{Ra} - Y_{Rb}}{Y_{Ra}} \times 100 \tag{5}$$

The cumulative precipitation slope change rate K_P is obtained similarly, then the contribution of precipitation to the runoff change C_P (%) is

$$C_P = |K_P/K_R| \times 100 \tag{6}$$

The anthropogenic contribution C_H (%) is $C_H = 100 - C_P$. The contribution of the two factors to sediment load can be similarly found by replacing runoff with sediment load following the above steps (Kong *et al.* 2018).

4. RESULTS

4.1. Runoff and sediment time-varying characteristics

In order to visualize the changes in runoff and sediment load in the Wei River mainstream, the runoff and sediment variation from 1971 to 2020 at the Huaxian station were plotted using multiyear runoff and sediment statistics (see Figure 2). The interannual variation of runoff volume from 1971 to the mid-1990s is large, with an average value of 6.58 billion m^3, and after the mid-1990s, the runoff volume becomes smaller and the interannual variation is relatively stable, with an average value of 5 billion m^3. The maximum and minimum values of annual runoff were 13.1 billion m^3 and 1.683 billion m^3, which occurred in 1983 and 1997, mainly related to the precipitation of that year. From the trend line, it can be seen that the overall trend of runoff is decreasing, with an average annual decrease of 62.9 million m^3. The maximum value of sediment load occurs in 1973, and the interannual variation is large until the mid-2000s, which is basically consistent with the variation trend of runoff volume, that is, large runoff with large sediment, small runoff with small sediment. From the mid-2000s onward, the variation of sediment load decreases and shows a clear downward trend. From the long-term trend, sediment load is on a decreasing trend, decreasing by 6.8 million tons per year on average.

The interannual variation graphs of runoff and sediment load at the Huaxian station are highly fluctuating and can only be analyzed qualitatively and with large errors by observation alone. In order to quantify the assessment, the M–K test was used

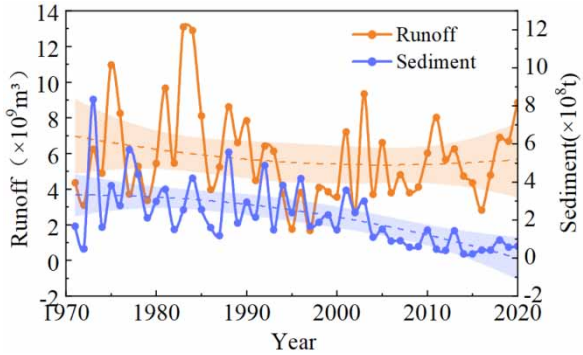

Figure 2 | Trends of annual runoff and sediment load in the Wei River.

to evaluate the trend of runoff and sediment load. The Z values of the test statistics for runoff and sediment load were calculated to be -0.44 and -4.99, and taking the significance level $\alpha = 0.05$, then $Z_{1-\alpha/2} = 1.96$, $|Z_{\text{runoff}}| = 0.44 < 1.96$, $|Z_{\text{sediment}}| = 4.99 > 1.96$. This indicates that there is no significant downward trend in multiyear runoff and a significant downward trend in multiyear sediment load at the 95% confidence level for the Huaxian station, which is basically consistent with the results of the visual analysis above.

4.2. Runoff and sediment situation variation identification

The results of the M–K mutation test are shown in Figure 3. When the curve exceeds the critical value, the upward or downward trend is significant. The multiyear runoff at the Huaxian station basically falls within the critical range, indicating that the rising and falling trend are not obvious. It shows a weak increasing trend from 1971 to 1995 and a weak decreasing trend after 1995. The intersection of the curves *UF* and *UB* is in 1991, which falls within the significant level, and the year of abrupt change is likely to be 1991. The multiyear sediment load shows an increasing trend from 1971 to 1986, and then basically stabilizes without any obvious trend of increase or decrease. After 1996, there was a decreasing trend, and after 2007, there was a significant decrease, and the decreasing trend has been increasing. The intersection of the two curves is in 2006, which is within the critical range and may be a sudden change year.

To determine the accuracy of the M–K method calculation results, the mean difference t-test was used to test whether the mutation year was reasonable. The significance level α is generally taken as 0.01 or 0.05, and to ensure the rigor of the test results, $\alpha = 0.01$, which means $t_\alpha = 2.704$. The calculated mutation index in annual runoff is 0.345, and the statistic $t = 2.439 < 2.704$, which indicates that at the significance level $\alpha = 0.01$, no significant mutation occurred in runoff in 1991, so we consider that 1991 did not represent a significant abrupt change. Therefore, we believe that there was no abrupt change in 1991. The mutation index in annual sediment load is 1.054, with the statistic $t = 4.824 > 2.704$, which indicates that at the significance level $\alpha = 0.01$, there is a mutation in sediment load in 2006.

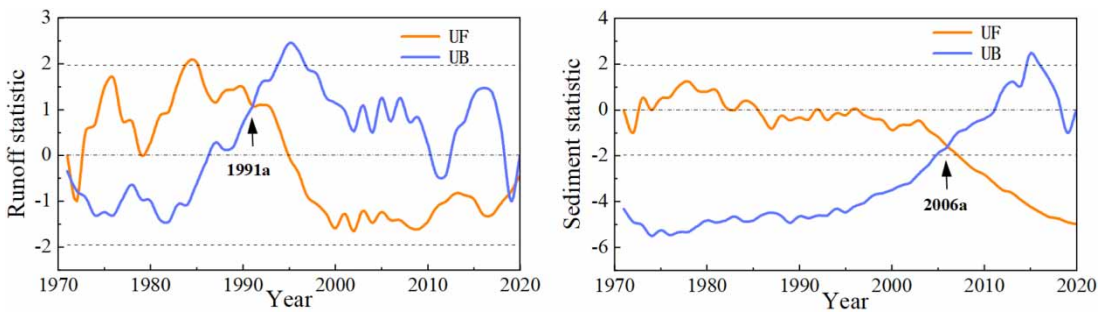

Figure 3 | Mann–Kendall statistics of runoff and sediment load.

4.3. Periodic fluctuations in runoff and sediment regime

4.3.1. Continuous wavelet analysis

The calculated multitimescale periodicity variation of runoff and sediment load is shown in Figures 4 and 5, with the red part being the abundant water area and the blue part being the dry water area. The wavelet variance plots show the amplitude of the periodicity vibration within the sequence; the larger the vibration amplitude, the more obvious the periodicity, which makes it convenient to find the dominant periodicity. As seen in Figure 4, the periodicity of runoff is more obvious. On the large time scale, there is variation periodicity of 23–32 years between 1971 and 2020, mainly experiencing the change from dry to abundant to dry to abundant to dry with a more stable periodicity. On the small time scale, before the 1990s, there were mainly variation periodicities of 9–15 years and 5–6 years, while after the 1990s, the short periodicity of 5–6 years gradually disappeared and the 9–15 years periodicity gradually changed to form the periodicities of 9–10 years and 11–15 years. The wavelet variance plots show that the main periodicities of runoff variation are 10 years, 12–13 years, and 29 years, with 12–13 years having the largest variance value and being the dominant periodicity of runoff variation, indicating that the periodicity of 12–13 years is the most pronounced in the WRB.

The periodicity of sediment load in Figure 5 is relatively chaotic and less stable and is less periodic compared with runoff. With the 1990s as the dividing line, the periodicity changes greatly before and after. Before the 1990s, the periodicity of sediment load was relatively strong, with three main periodicities of 4–5 years, 7–8 years, and 18–24 years. However, after the 1990s, the periodicity gradually changed, and the 18–24 years periodicity gradually changed to 20–23 years, and the short periodicities of 4–5 years and 7–8 years gradually weakened and disappeared, as well as the emergence of a new periodicity of 12–14 years. The periodicity generally becomes longer and weaker in this period. From the wavelet variance diagram, it can be seen that the more obvious periodicities of sediment load are 3 years, 5 years, and 22 years, among which 5 years has the highest peak variance and is the dominant periodicity of sediment. Both runoff and sediment load changed around the 1990s, mainly because many water conservation projects were built in the Wei River in the 1970s and 1980s, and the runoff and sediment load tended to stabilize through runoff and sediment transfer, so the short periodicities of

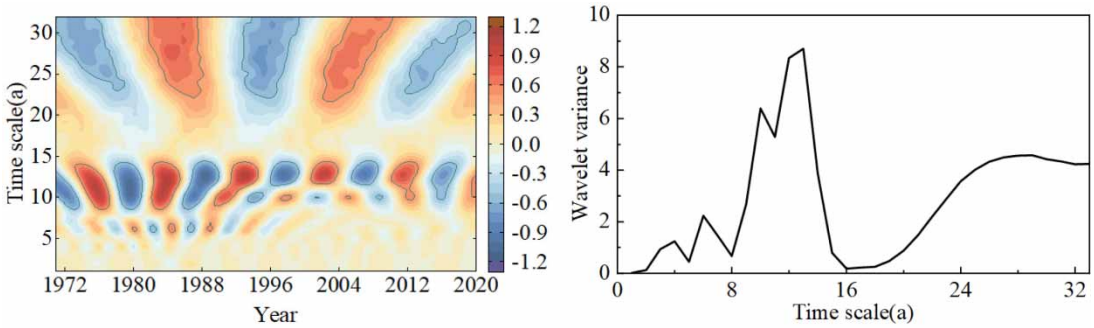

Figure 4 | Wavelet analysis diagram of the Wei River runoff.

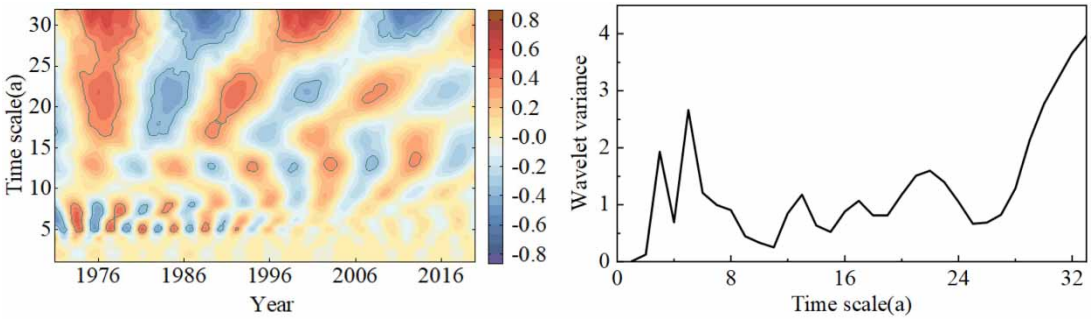

Figure 5 | Wavelet analysis of sediment load in the Wei River.

both began to disappear in the late 1980s, leaving only a few longer periodicities. Sediment load is more influenced by human activities, and the periodicity is relatively weak.

4.3.2. Synergistic evolution of runoff and sediment

Cross-wavelet analysis is used to analyze the correlation details of runoff and sediment load on the cycle at multiple scales. The cross-wavelet includes the cross-wavelet power spectrum and coalescence spectrum, which can analyze significant correlations in high- and low-energy regions. The phase spectrum is represented by arrows, which can be well combined with the power and coalescence spectra, and the results are shown in Figure 6. The thin black conical line in the figure is the cone of influence of the wavelet; the gray part outside the curve is not considered because of edge effects; and the thick black solid line indicates that the enclosed area passes the 95% red noise test. The arrows are vectors, representing the phase difference between two time series. The horizontal rightward arrow '→' has a phase angle of 0°, indicating a positive phase relationship between runoff and sediment load; while the leftward arrow '←' has a phase angle of 180°, indicating a negative phase relationship; the arrow '↑' indicates that the runoff is 1/4 period ahead of the sediment load, and '↓' indicates that the runoff is 1/4 period behind the sediment load.

The power spectrum in Figure 6 shows a weak correlation between runoff and sediment in general, with few resonant periodicities. The two resonance periods that passed the test are all before 1995. The period 1971–1976 has a significant 0–2 years resonance periodicity between runoff and sediment, and since this time periodicity is partly in the region affected by edge effects, only the period 1974–1976 is considered, with a phase angle of 0°, indicating a positive correlation between runoff and sediment. The period 1980–1990 has a significant resonance periodicity of 3–5 years, with a phase angle of −45°, and the runoff is delayed by 1/8 period compared with the sediment load, which is roughly positively correlated. The resonance periodicity in the coalescence spectrum is mainly concentrated in the periodicities of 0–2 years from 1996 to 2005, 3–5 years from 2005 to 2014, and 9–12 years from 2005 to 2019. Since the 9–12a cycle is outside the influence cone, this cycle is not considered. Among them, the ones that passed the test are the 0–1.5 years periodicity from 2002 to 2005 with a phase angle of 0°, which is positively correlated, and the 3–5 years periodicity from 2005 to 2014 with a phase angle of 90°, where the runoff is 1/4 period ahead of the sediment load. In summary, the runoff–sediment resonance periodicity in the Wei River is small, and overall the interaction between the two is small and the consistency is weak. However, the resonance effect of runoff–sediment is better in some time periods, mainly concentrated in the 1980s and 2000s. Higher rainfall in the 1980s, and 1983 and 1984 were still the highest rainfall years, led to increased runoff and an impact on river siltation and a consequent increase in river sediment load. The precipitation periodicity of 3–5 years coincides with the greater significance of the 3–5 years periodicity of runoff and sediment between 1980 and 1990. The lower reaches of the Wei River experienced the '03·8', '03·10', '05·10', and '11·09' major floods, which were in a scouring state, coinciding with the significant periodicity of runoff and sediment during 2002–2014.

4.4. Runoff and sediment relationship in different periods

The relationship line is drawn with the cumulative runoff and cumulative sediment load as the horizontal and vertical coordinates, and the double cumulative curve of runoff and sediment load at the Huaxian station is shown in Figure 7. The cumulative runoff and cumulative sediment load show a good linear relationship. When the curve is a straight line, the runoff–sediment relationship in the time period does not change greatly and is maintained in a relatively balanced state; if

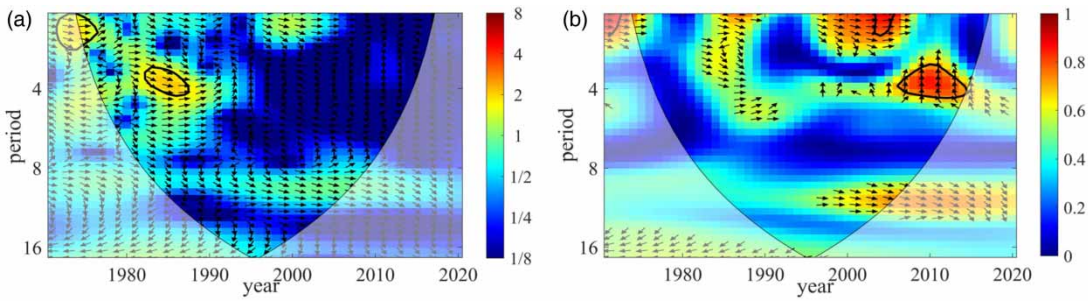

Figure 6 | Cross-wavelet power spectrum (a) and coalescence spectrum (b) of runoff and sediment.

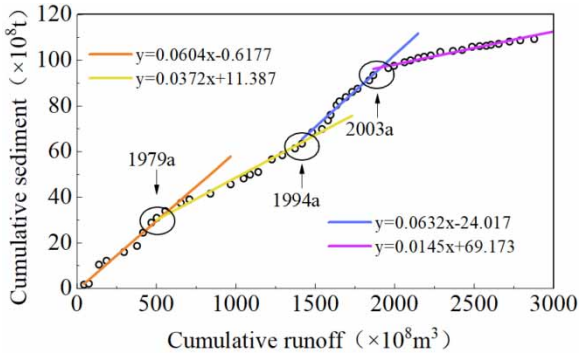

Figure 7 | Double accumulation curve of runoff–sediment.

the curve has an inflection point and the slope of the line changes, it means that the runoff–sediment relationship changes after the time at the inflection point and reaches another balanced state. Most of the reasons for the change in slope are climatic factors or human activities. The obvious slope change in the position on the runoff–sediment curve for 1979, 1994, and 2003 allows the runoff–sediment time series in the WRB to be divided into four stages: 1971–1979, 1980–1994, 1995–2003, and 2004–2020, and the mean values of runoff–sediment for each stage are calculated, as shown in Table 1. Taking the runoff–sediment relationship from 1971 to 1979 as the reference period, the slope of the period from 1980 to 1994 became smaller. Because the sediment load reduced and runoff increased at this stage, the runoff–sediment relationship shifted to 'more runoff and less sediment.' The main reason is that the systematic construction of runoff conservancy projects began in the 1970s. The second inflection point was around 1994, and the slope of the curve became larger in the period 1995–2003. From the average value, it can be seen that the change in sediment load in this stage is small, but because the runoff is reduced by 2.965 billion m^3 compared with the second stage, the sediment is relatively increased, so the relationship between runoff and sediment in this stage changes to 'less runoff and more sediment'. The slope of the 2004–2020 period decreases, and the slope changes more compared with the third period. The amount of sediment load decreases significantly during this period, and the runoff–sediment relationship between changes to 'more runoff and less sediment', which is mainly related to many soil and water conservation policies carried out by the country in the 21st century.

4.5. Impacts of climate change and human activities

The factors that can affect the change of runoff and sediment are mainly divided into two categories: climate factors and human activities factors. Precipitation is the dominant climate factor, so it is used to represent the climate factor in this paper. Calculating the contribution rate of precipitation and human activities to runoff–sediment can reveal the degree to which changing factors influence runoff–sediment. The cumulative curves of runoff, sediment, and precipitation are shown in Figure 8. Both the cumulative runoff and cumulative precipitation curves were deflected in 1994, indicating that the trends in precipitation and runoff are in good agreement. Both changed after that point in time, while the deflection of the runoff curve was greater than that of precipitation, probably due to the increased influence of human activities on runoff changes. By comparing the slope before and after the change, the contribution of precipitation and human activities to the change of runoff is 21.2 and 78.8%, so it is human activities that have the greatest influence on the measured runoff. The deflection of the cumulative sediment load curve occurred in 2003, which is weakly consistent with the precipitation variation. The contribution of precipitation to sediment load was calculated to be only 4.7%, while the contribution of human activities was as high as 95.3%, further confirming the low correlation between sediment load and precipitation.

Table 1 | Average values of runoff and sediment in different periods

Category	1971–1979	1980–1994	1995–2003	2004–2020
R ($\times 10^8$ m^3)	55.75	71.83	42.18	54.07
S ($\times 10^8$ ton)	3.44	2.86	2.53	0.76

Note: R is the mean runoff; *S* is the mean sediment load.

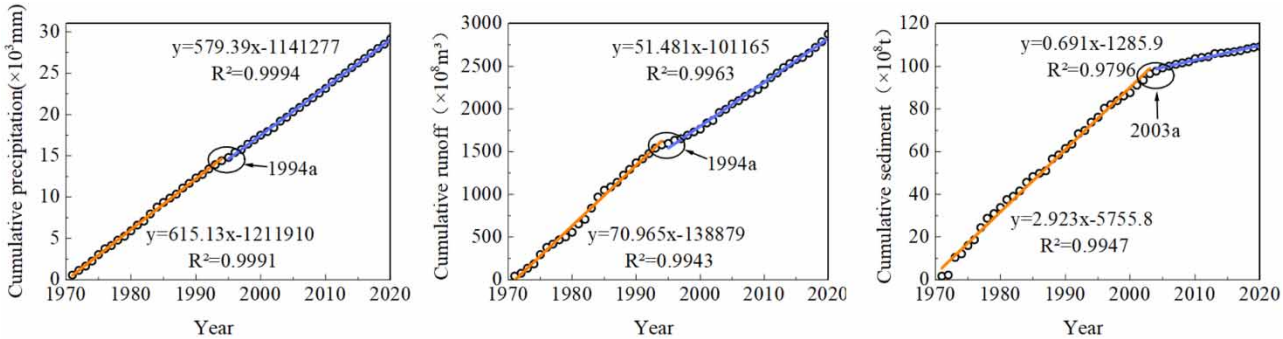

Figure 8 | Accumulation curves of runoff, sediment load, and precipitation.

Taken together, the impact of human activity on both is much higher than the impact of climate, so the factor of human activities dominates in runoff–sediment change. Among them, the degree of influence of human activities on sediment load is higher than that on runoff, and the amount of sediment load is more closely related to human activities.

5. DISCUSSION

5.1. Relationship between precipitation and evolution of runoff and sediment

Precipitation in the WRB is unevenly distributed in time, and the effect of precipitation on runoff–sediment variability differs at different time periods. The linear correlations of precipitation with runoff and sediment load for the four time periods are shown in Figure 9. From the distribution of data points and trend lines, it can be seen that the correlation of runoff in each period is significant, while the correlation of sediment load is not significant except for the period from 1980 to 1994. The linear correlation between runoff and precipitation is much larger than that between sediment load and precipitation, indicating that the runoff volume is more influenced by precipitation, and that there are other external factors besides precipitation in the variation of sediment load, of which human activities account for a large part. Precipitation and runoff show a significant positive correlation. The amount of precipitation before 1994 was high, and a large amount of precipitation formed runoff through the production and confluence stages, which did not require much intervention except for the necessary flood regulation, so the correlation between runoff and rainfall was highest in this period. The correlation between runoff and precipitation is getting lower and lower because there has been a significant decrease in precipitation since 1994, the temperature increases by 0.2 °C per year after the 1990s, and the runoff volume decreased after infiltration through evaporation, which requires human intervention such as reservoir scheduling to redistribute runoff (Li *et al.* 2019).

The amount of sediment load mainly depends on the soil condition and the construction of water conservancy projects in the basin, and precipitation can only affect it indirectly through runoff, so the linear correlation between sediment load and precipitation is very weak and not significant in most periods. Only in 1980–1994, the correlation between precipitation and

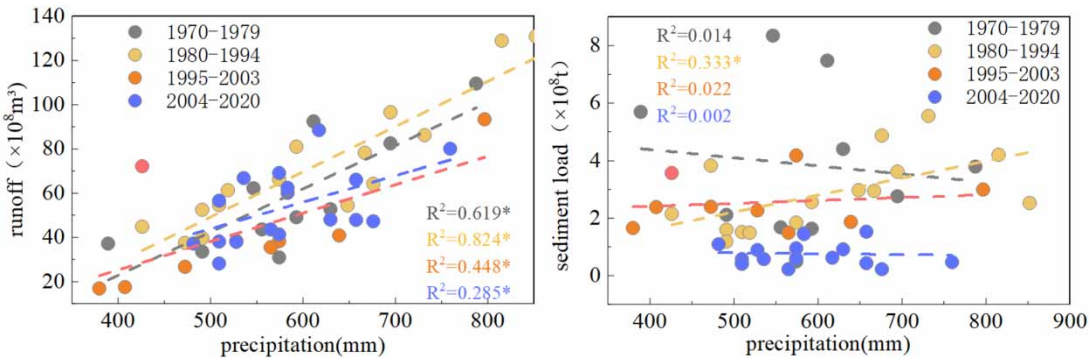

Figure 9 | Linear relationship between precipitation and runoff–sediment (* means $p < 0.05$, R^2 passed the significance test with confidence of 95%, and there is a significant correlation between them).

sediment load is relatively high and $p < 0.05$, indicating that there is a significant correlation between precipitation and sediment during this period. This is mainly due to the high runoff volume in that period, which has an impact on river sediment and leads to higher sediment content in the river as it is washed downstream along with the river. Both runoff and sediment load were best correlated with precipitation in the time period 1980–1994. During this time period, precipitation has an important relationship with the change of runoff and sediment, giving some consistency in runoff and sediment load. Although the correlation between precipitation and sediment load is poor, some studies show that rainfall intensity has a great influence on sediment load. The Loess Plateau has loose soil, weak anti-erosion ability and is easily washed by rain. Therefore, the greater the rainfall intensity, the more serious the soil erosion, which leads to the increase of river sediment load. The WRB is located in the Loess Plateau, and its tributary Jing River is located in the sediment-producing area. Rainfall intensity will have a great impact on the sediment load of the Wei River. However, when the rainfall intensity exceeds a certain threshold, the sediment load will not increase with the increase of rainfall intensity. The vegetation coverage rate will affect the threshold, and the higher the vegetation coverage rate, the higher the threshold (Liu *et al.* 2020).

5.2. Impact of human activities

5.2.1. The underlying surface changes in the basin

Land use can directly reflect the status of human exploitation of land and land change over the years (Wagner *et al.* 2019). The years 1980, 1990, 1995, 2000, 2005, 2010, 2015, and 2020 were selected as representative years. The land use type data for these years was statistically calculated and the results are shown in Figure 10. The WRB is dominated by cultivated land, mostly distributed in the eastern part of the gently sloping terrain, which can reach about half of the total area. This is followed by forest land and grassland, with the sum of the three accounting for about 94% of the total. The area of cultivated land changed the most during the last 40 years. Compared with 1980, the area of cultivated land decreased by 3,384 km^2 in 2020. After entering the 21st century, the rate of decline of cultivated land accelerated due to policy requirements and changes in the focus of people's lives, and the reduced areas were basically in this period. Social and technological developments and population growth in recent years have seen the population of the WRB grow to 39.44 million people, as of 2016. This has necessitated the reclamation of more land to meet the growing needs of the population, resulting in the expansion of the building land area by 1,840 km^2, an increase of as much as 66%. After 1995, forest land showed an obvious growth trend, while grassland area tended to be stable and increased rapidly after 2015. But during the 1990s, the area of both showed substantial fluctuations. The increase of grassland and the decrease of forest land in the early period were due to the acts of over-cultivation and development after the improvement of technology, and the normal standard of grassland and forest land was restored after the awareness of the importance of ecological protection in the later period. The watershed area changed a lot around 2000. It has been on a decreasing trend during the 1980s and 1990s. After 2000, the rivers and lakes began to be treated, and the watershed area increased. After 2005, the area had ups and downs but roughly stabilized. The unused area is less and the overall trend is decreasing, so it will no longer be analyzed.

Most of the land use changes were concentrated in the period of 1990–2005, and the statistics of the transition between land types in this period are shown in Figure 11. In the 1990s, the annual precipitation was only about 500 mm, which was in the dry period, while human water consumption increased significantly. A large amount of groundwater was extracted,

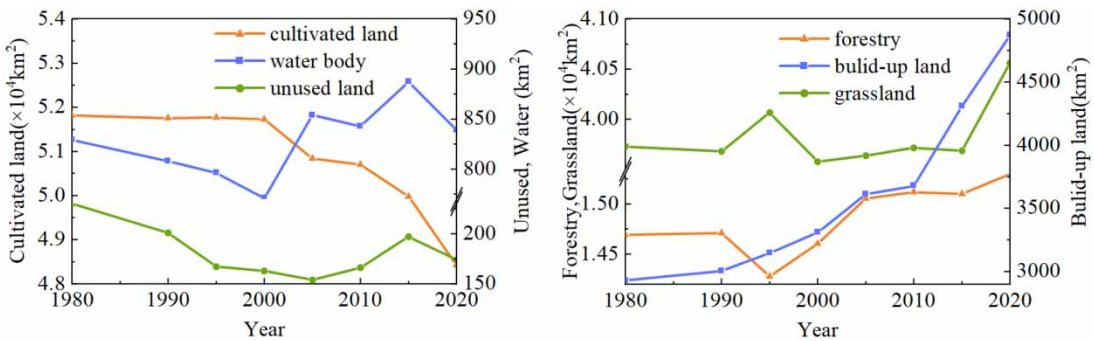

Figure 10 | Area change of land types in WRB in 1980–2020.

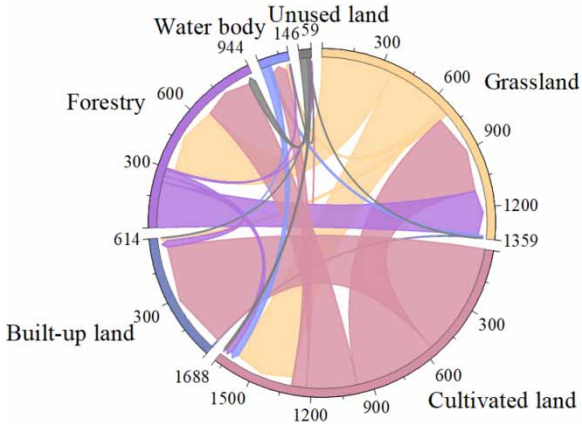

Figure 11 | Transition of land types during 1990–2005. The figure shows the transfer of land types from 1990 to 2005. For example, the arrow from A to B indicates that A is converted into B, and the thickness of the arrow indicates the conversion area. In the figure, the area of land type that has not been transformed has been deleted, and the transfer part between land types can be seen more intuitively.

and water consumption increased from 2.793 billion m^3 before 1990 to 4.263 billion m^3, so the water area continued to decrease, which is mainly converted into cultivated land. In addition, from 1990 to 1995, indiscriminate logging led to the loss of 430 km^2 of forest land, which was mainly converted into grassland, resulting in serious soil erosion. This is the reason why the runoff–sediment relationship changed in the direction of 'less runoff and more sediment' around 1994. In 1999, the country started to implement the policy of returning farmland to forest and grass, which accelerated the transformation of cultivated land to forest and grassland, and people's subsistence development occupied part of the cultivated land, so the rate of decline of cultivated land area accelerated after 2000, mainly transforming into built-up land, grassland, water body, and forest. The increase in forest land has improved the soil erosion problem to some extent, and coupled with the fact that preparations for the comprehensive management of the WRB had begun in 2002 and *the measures of the Key Management Plan for the WRB* were formally introduced in 2005, the soil and water conservation projects have covered 20,691 km^2 of the main river basin, accounting for 30.8% of the WRB area, as of 2010 (Huang *et al.* 2021). Therefore, the decrease in sediment load since 2002 is a turning point in the change of the runoff–sediment relationship.

The Pearson correlation coefficient method was used to judge the impact of land types on runoff and sediment load, and their correlation was further analyzed. The area of unused land is less than 0.4%, which has negligible influence, and the error in the calculation is large, so it is not substituted into the calculation. Land use data for 1980, 1990, 1995, 2000, 2005, 2010, 2015, and 2020 and runoff and sediment load for corresponding years were used to calculate correlation coefficients. The calculation results are shown in Table 2. The correlation is strongest when the absolute value of the correlation coefficient tends to 1, and weakest when it tends to 0. The correlation between grassland and runoff–sediment is extremely small and the effect is negligible. As a whole, the correlation between sediment load and land type is above 0.5 in absolute value and is significant except for grassland and water body. Hence, the influence of sediment load from subsurface changes is greater, which is consistent with the above contribution. The correlation between runoff and all land use types is not significant. The underlying surface does not directly determine the runoff volume but only indirectly influences the runoff variation from the side. The correlation coefficient of forest land is the highest, which is 0.618, because forest land can promote the conversion of groundwater to rivers and has a recharge effect on runoff (Li *et al.* 2018). The ground permeability of

Table 2 | Correlation coefficient between land use types and runoff and sediment

		Cultivated	Forest	Grassland	Water	Built-up
Runoff	R	−0.493	0.618	0.374	0.247	0.345
	p	0.215	0.102	0.362	0.555	0.403
Sediment	R	0.810	−0.815	−0.271	−0.695	−0.860
	p	0.015	0.014	0.516	0.056	0.006

Note: R is the correlation coefficient, when $p < 0.05$, the correlation is significant, when $p > 0.05$, the correlation is not significant

built-up land is poor, resulting in less rainwater infiltration and increased ground flow production capacity, so it has a positive correlation with runoff, with a correlation coefficient of 0.345, which has a weak effect on runoff. The large reduction in cultivated land is converted to forested land and built-up land that will recharge runoff, so cultivated land has an indirect negative correlation with runoff, with a correlation coefficient of −0.493.

There is a significant negative correlation between sediment load and forest and building land. Forests reduce rainfall intensity through their canopy, thus slowing down the impact of rainfall on the ground, and the root system also consolidates the soil (Han *et al.* 2021). Buildup sites generally cover the land with construction materials such as cement, which prevents the erosion of the land by foreign objects and has the highest correlation with the change of sediment load. Both of the above reduce the amount of sediment load by the river from the source, with correlation coefficients of −0.815 and −0.860. The correlation between cultivated land and sediment load is positive, mainly because the root system of crops in cultivated land is shallow, which cannot consolidate the soil well, and it is easy to cause soil erosion. In addition, it is indirectly affected by the conversion of forest land, water area, and construction land, and the correlation coefficient is 0.810.

It is worth mentioning that terraced fields have a great impact on sediment load. In the document on soil and water conservation in the Yellow River Basin issued by the government, it is proposed that northern Shaanxi and other places should vigorously carry out terraced fields to reduce soil erosion. From 1980 to 2020, the terraced fields in WRB increased from 192 to 315 km^2, and the correlation coefficient with sediment load was −0.683, showing a significant negative correlation. Since the 1970s, the construction of terraced fields has reduced the sediment deposition in the upper and middle reaches of the Wei River by 101 million tons and 66 million tons (Liu *et al.* 2021b). From 2000 to 2015, the control efficiency of terraced fields on soil erosion increased from 0.263 to 0.365 (Wang *et al.* 2019). Compared with terraced fields on runoff, terraced fields have a greater impact on sediment load and remain stable all the time. When the land is seriously degraded or in the initial stage of restoration, terraced fields have a more significant impact on soil and water conservation (Wang & Yao 2019). Although terraced fields are a kind of cultivated land, their overall influence is opposite to that of cultivated land. This is because the stepped construction style can effectively slow down the velocity and kinetic energy of slope runoff by shortening the slope length, and the sediment can be intercepted to a certain extent (Chen & Yang 2011). However, terraced fields occupy a small area in cultivated land, accounting for only about 0.5%, so there is a positive correlation between cultivated land and sediment load as a whole.

5.2.2. Many water conservancy projects have been built

Hydraulic projects are the main means by which people regulate rivers and have a direct impact on runoff–sediment changes. A large number of hydraulic projects have been built and put into operation since the 1970s, and as of 2015, 1,635 diversion projects and more than 700 large check dams have been built in the WRB, most of which were constructed after 2000 (Chang *et al.* 2016). The Dongfanghong Irrigation Project, the Jiaokou Pumping Irrigation Project, the Baojixia Main Canal, and the expanded Luohui Canal that operated in the 1970s, together with some small- and medium-sized irrigation projects, brought the total irrigated area to 5,900 km^2. The significant water withdrawal from the river has resulted in a 34.5 m^3/s average annual runoff decrease, or 28% of the overall runoff reduction. In addition to transferring and storing water, Fengjiashan Reservoir and Shitouhe Reservoir in the 1980s also intercepted a large amount of sediment and reduced sediment by an average of 6.78 million tons per year in the 1980s compared with the 1970s. Reservoir storage increases the water area, resulting in greater evaporation, which also has an impact on runoff. In addition to this, studies have shown that the Sanmenxia Reservoir, although not located in the WRB, has had a serious impact on the runoff and sedimentation of the Wei River (Zhang *et al.* 2020). The Sanmenxia Reservoir raised the water level by more than 30 m due to power generation, slowing down the flow of the Wei River as it merges into the Yellow River, resulting in the lower reaches of the Wei River becoming seriously silted up, which raised the elevation of Tongguan by 4.7 m in only two years of operation. The allowable flow rate decreased from 5,500 m^3/s before the construction of the reservoir to 1,000 m^3/s after 1990, which was one of the main reasons for the major flood disaster of the Wei River in 2003 (Liu *et al.* 2022). To alleviate sedimentation in the lower reaches of the Wei River, the construction of the Dongzhuang Reservoir began in 2018 in the lower reaches of the Jing River, which is expected to intercept 750 million tons of sediment from tributaries to alleviate the burden on the lower reaches of the mainstream and is a key water conservation project in Shaanxi in recent years.

5.2.3. Influence of human water intake

After the reform and opening up, the economy of WRB has increased rapidly, and with the continuous growth of population, the industrial water consumption, agricultural water consumption, and domestic water consumption have increased

dramatically. Human water consumption becomes an important factor in the reduction of runoff in the Wei River, and some sediment will be taken away when taking water, which indirectly affects sediment load. According to statistics, the average water consumption of WRB was 2.793 billion m^3 before the 1990s, and the average water consumption increased to 4.263 billion m^3 in the 1990s, with an increase of 52.6%. The increase of water consumption is mainly manifested in the over-exploitation of groundwater, which affects the surface runoff. The increase of water consumption leads to the decrease of 864 million m^3 of the Yellow River inflow in WRB, accounting for 21% of the actual decrease of the Yellow River inflow in the 1990s. Water consumption for soil and water conservation increased by 184 million m^3 in the 1990s, accounting for 4% of the actual decrease of water inflow into the Yellow River in the 1990s (Xu *et al.* 2023).

6. CONCLUSION

- Runoff and sediment trends and abrupt change years in the Wei River mainstream basin are significantly different. There is no obvious trend change and abrupt change in runoff. While the sediment delivery shows a significant decreasing trend, the abrupt change in sediment delivery occurs around 2006. The runoff volume is dominated by long periodicity, with the main periodicities of 10a, 12–13a, and 29a, and 12–13a is the dominant periodicity. The periodicity of sediment load does not have obvious consistency with the runoff periodicities, mostly with shorter periodicity. The main periodicities are 3a, 5a, and 22a, with 5a as the dominant periodicity.
- In the high-energy region, there is a significant resonance periodicity of 3–5a in 1980–1990, which is roughly positively correlated. In the low-energy region, the main resonance periodicities are 0–1.5a in 2002–2005, which are positively correlated, and 3–5a in 2005–2014. The runoff–sediment sequence can be divided into four stages: 1971–1979, 1980–1994, 1995–2003, and 2004–2020, and the runoff–sediment relationship changes significantly at the time points of 1979, 1994, and 2003.
- The contribution of precipitation and human activities to runoff is 21.2 and 78.8%, and the contribution to sediment load is 4.7 and 95.3%, so human activities are the main factors of runoff and sediment change.

AUTHOR CONTRIBUTIONS

W.G. contributed to funding acquisition; project administration; resources; investigation; supervision. Y.S. contributed to conceptualization; data curation; formal analysis; investigation; methodology; resources; software; validation; visualization; writing – original draft, writing – review and editing. J.H. contributed to investigation; formal analysis; methodology; validation; visualization. W.W. contributed to visualization; investigation; formal analysis. H.W. contributed to funding acquisition; project administration.

FUNDING

This study was supported by the National Natural Science Fund of China (51779094), the 2016 Henan University Science and Technology Innovation Talent Support Plan (16HASTIT024), the Guizhou Provincial Water Resources Department 2020 Water Conservancy Science and Technology Project (KT202008), and the Basic Research Project of Key Scientific Research Projects of Colleges and Universities of Henan Province (23ZX012).

DATA AVAILABILITY STATEMENT

Data cannot be made publicly available; readers should contact the corresponding author for details.

CONFLICT OF INTEREST

The authors declare there is no conflict.

REFERENCES

Ay, M. & Kisi, O. 2017 Trend analysis of streamflows at some gauging stations over the Kizilirmak River. *Teknik Dergi* **28** (2), 7779–7794. doi:10.18400/tekderg.304034.

Brierley, G. & Fryirs, K. 2022 Truths of the riverscape: moving beyond command-and-control to geomorphologically informed nature-based river management. *Geoscience Letters* **9** (1). doi:10.1186/s40562-022-00223-0.

Chang, J. X., Li, Y. Y., Wei, J., Wang, Y. M. & Guo, A. J. 2016 Dynamic changes of sediment load and water discharge in the Weihe River, China. *Environmental Earth Sciences* **75** (12). doi:10.1007/s12665-016-5841-9.

Chen, R. S. & Yang, K. H. 2011 Terraced paddy field rainfall-runoff mechanism and simulation using a revised tank model. *Paddy and Water Environment* **9** (2), 237–247. doi:10.1007/s10333-010-0225-3.

Deng, W. J., Song, J. X., Bai, H., He, Y., Yu, M., Wang, H. Y. & Cheng, D. D. 2018 Analyzing the impacts of climate variability and land surface changes on the annual water-energy balance in the Weihe River Basin of China. *Water* **10** (12). doi:10.3390/w10121792.

Durocher, M., Lee, T. S., Ouarda, T. & Chebana, F. 2016 Hybrid signal detection approach for hydro-meteorological variables combining EMD and cross-wavelet analysis. *International Journal Of Climatology* **36** (4), 1600–1613. doi:10.1002/joc.4444.

Fan, J. J., Xu, F. F., Sun, X., Dong, W., Ma, X. J., Liu, G. P., Cheng, Y. & Wang, H. 2022 Construction and application of hydrometeorological comprehensive drought index in Weihe River. *Atmosphere* **13** (4). doi:10.3390/atmos13040610.

Ghaderpour, E., Ince, E. S. & Pagiatakis, S. D. 2018 Least-squares cross-wavelet analysis and its applications in geophysical time series. *Journal of Geodesy* **92** (10), 1223–1236. doi:10.1007/s00190-018-1156-9.

Gocic, M. & Trajkovic, S. 2013 Analysis of changes in meteorological variables using Mann-Kendall and Sen's slope estimator statistical tests in Serbia. *Global And Planetary Change* **100**, 172–182. doi:10.1016/j.gloplacha.2012.10.014.

Guo, T. T., Zhang, T. P., Lim, E., Lopez-Benitez, M., Ma, F. & Yu, L. M. 2022 A review of wavelet analysis and its applications: challenges and opportunities. *IEEE Access* **10**, 58869–58903. doi:10.1109/access.2022.3179517.

Han, D. D., Deng, J. C., Gu, C. J., Mu, X. M., Gao, P. & Gao, J. J. 2021 Effect of shrub-grass vegetation coverage and slope gradient on runoff and sediment yield under simulated rainfall. *International Journal Of Sediment Research* **36** (1), 29–37. doi:10.1016/j.ijsrc.2020.05.004.

Huang, S. Z., Liu, D. F., Huang, Q. & Chen, Y. T. 2016 Contributions of climate variability and human activities to the variation of runoff in the Wei River Basin, China. *Hydrological Sciences Journal* **61** (6), 1026–1039. doi:10.1080/02626667.2014.959955.

Huang, C. L., Yang, Q. K. & Huang, W. D. 2021 Analysis of the spatial and temporal changes of NDVI and Its driving factors in the Wei and Jing River Basins. *International Journal of Environmental Research and Public Health* **18** (22). doi:10.3390/ijerph182211863.

Jiang, C., Xiong, L. H., Wang, D. B., Liu, P., Guo, S. L. & Xu, C. Y. 2015 Separating the impacts of climate change and human activities on runoff using the Budyko-type equations with time-varying parameters. *Journal of Hydrology* **522**, 326–338. doi:10.1016/j.jhydrol.2014.12.060.

Kong, B., Huang, S. Z., Ma, L. & Huang, Q. 2018 Spatio-temporal changes in potential evaporation and possible causes based on SCRAQ method: a case study in the Wei River Basin, China. *Journal of Coastal Research*, 94–102. doi:10.2112/si84-014.1.

Li, B. Q., Xiao, W. H., Wang, Y. C., Yang, M. Z. & Huang, Y. 2018 Impact of land use/cover change on the relationship between precipitation and runoff in typical area. *Journal of Water and Climate Change* **9** (2), 261–274. doi:10.2166/wcc.2018.055.

Li, C., Zhang, H. B., Gong, X. H., Wei, X. W. & Yang, J. T. 2019 Precipitation trends and alteration in Wei River Basin: implication for water resources management in the transitional zone between plain and Loess Plateau, China. *Water* **11** (11), 2407–2424. doi:10.3390/w11112407.

Li, L., Ni, J. R., Chang, F., Yue, Y., Frolova, N., Magritsky, D., Borthwick, A. G. L., Ciais, P., Wang, Y. C. & Walling, D. E. 2020a Global trends in water and sediment fluxes of the world's large rivers. *Science Bulletin* **65** (1), 62–69. doi:10.1016/j.scib.2019.09.012.

Li, Y. T., Cai, Y. P., Li, Z., Wang, X., Fu, Q., Liu, D., Sun, L. & Xu, R. H. 2020b An approach for runoff and sediment nexus analysis under multi-flow conditions in a hyper-concentrated sediment river, Southwest China. *Journal Of Contaminant Hydrology* **235**, 103702–103712. doi:10.1016/j.jconhyd.2020.103702.

Liu, X. Y., Dang, S. Z., Liu, C. M. & Dong, G. T. 2020 Effects of rainfall intensity on the sediment concentration in the Loess Plateau, China. *Journal of Geographical Sciences* **30** (3), 455–467. doi:10.1007/s11442-020-1737-4.

Liu, D., Wang, X., Jaramillo, F., Yi, Y. J., Li, C. H. & Yang, Z. F. 2021a A probabilistic conceptual model to attribute runoff variations to human activity. *Hydrological Sciences Journal-Journal Des Sciences Hydrologiques* **66** (2), 309–321. doi:10.1080/02626667.2020.1857387.

Liu, W., Shi, C. X., Ma, Y. Y., Li, H. J. & Ma, X. Q. 2021b Land use and land cover change-induced changes of sediment connectivity and their effects on sediment yield in a catchment on the Loess Plateau in China. *Catena* **207**, 105688–105698. doi:10.1016/j.catena.2021.105688.

Liu, J., Wang, P., Chen, X. Q., Shi, W., Song, L. J. & Hu, J. M. 2022 The changes in drainage systems of Weihe Basin and Sanmenxia Basin since late pliocene give new insights into the evolution of the Yellow River. *Frontiers in Earth Science* **9**. doi:10.3389/feart.2021.820674.

Mikhailov, V. N. 2010 Water and sediment runoff at the Amazon River mouth. *Water Resources* **37** (2), 145–159. doi:10.1134/s009780781002003x.

Sang, Y. F., Singh, V. P., Sun, F. B., Chen, Y. N., Liu, Y. & Yang, M. Y. 2016 Wavelet-based hydrological time series forecasting. *Journal of Hydrologic Engineering* **21** (5). doi:10.1061/(asce)he.1943-5584.0001347.

Schnitzer, S., Seitz, F., Eicker, A., Guntner, A., Wattenbach, M. & Menzel, A. 2013 Estimation of soil loss by water erosion in the Chinese Loess Plateau using universal soil loss equation and GRACE. *Geophysical Journal International* **193** (3), 1283–1290. doi:10.1093/gji/ggt023.

Shen, C. & Qiang, H. 2014 Spatial and temporal variation of annual precipitation in a river of the Loess Plateau in China. *Journal of Applied Mathematics* **2014**, 1–11. doi:10.1155/2014/827120.

Shi, C. X., Zhang, L. A., Xu, J. Q. & Guo, L. P. 2010 Sediment load and storage in the lower Yellow River during the late holocene. *Geografiska Annaler Series A – Physical Geography* **92A** (3), 297–309. doi:10.1111/j.1468-0459.2010.00396.x.

Song, J. & Liu, H. Z. 2020 Enlightenment and influence of water control elements in traditional literary works on modern river overflow control. *Journal of Coastal Research* **104**, 849–853. doi:10.2112/jcr-si104-145.1.

Song, J. X., Xu, Z. X., Hui, Y. H., Li, H. E. & Li, Q. 2010 Instream flow requirements for sediment transport in the lower Weihe River. *Hydrological Processes* **24** (24), 3547–3557. doi:10.1002/hyp.7780.

Tian, S. M., Xu, M. Z., Jiang, E. H., Wang, G. H., Hu, H. C. & Liu, X. 2019 Temporal variations of runoff and sediment load in the upper Yellow River, China. *Journal of Hydrology* **568**, 46–56. doi:10.1016/j.jhydrol.2018.10.033.

Tian, P., Liu, L., Tian, X. J., Zhao, G. J., Klik, A., Wang, R. D., Lu, X. Y., Mu, X. M. & Bai, Y. P. 2022 Sediment yields variation and response to the controlling factors in the Wei River Basin, China. *Catena* **213**, 106181–106193. doi:10.1016/j.catena.2022.106181.

Wagner, P. D., Bhallamudi, S. M., Narasimhan, B., Kumar, S., Fohrer, N. & Fiener, P. 2019 Comparing the effects of dynamic versus static representations of land use change in hydrologic impact assessments. *Environmental Modelling & Software* **122**, 1–9. doi:10.1016/j.envsoft.2017.06.023.

Wang, Y. F. & Yao, S. B. 2019 Effects of restoration practices on controlling soil and water losses in the Wei river catchment, China: an estimation based on longitudinal field observations. *Forest Policy and Economics* **100**, 120–128. doi:10.1016/j.forpol.2018.12.001.

Wang, Y. F., Zhang, T. T., Yao, S. B. & Deng, Y. J. 2019 Spatio-temporal evolution and factors influencing the control efficiency for soil and water loss in the Wei river catchment, China. *Sustainability* **11** (1), 216–239. doi:10.3390/su11010216.

Wang, B., Wang, H., Zeng, X. F. & Li, B. J. 2022 Towards a better understanding of social-ecological systems for basin governance: a case study from the Weihe River Basin, China. *Sustainability* **14** (9), 4922–4932. doi:10.3390/su14094922.

Xu, F., Zhao, Y. W., Yang, Z. F. & Zhang, Y. 2011 Multi-scale evaluation of river health in Liao River Basin, China. *Frontiers of Environmental Science & Engineering in China* **5** (2), 227–235. doi:10.1007/s11783-010-0219-9.

Xu, R., Gu, C., Qiu, D., Wu, C., Mu, X. & Gao, P. 2023 Analysis of runoff changes in the Wei River Basin, China: confronting climate change and human activities. *Water* **15** (11), 2081–2098. doi:10.3390/w15112081.

Ye, X. C., Xu, C. Y. & Zhang, Z. X. 2020 Comprehensive analysis on the evolution characteristics and causes of river runoff and sediment load in a mountainous basin of China's subtropical plateau. *Journal of Hydrology* **591**, 125597–125608. doi:10.1016/j.jhydrol.2020.125597.

Zhang, X. D. 2010 Strictly standardized mean difference, standardized mean difference and classical t-test for the comparison of two groups. *Statistics in Biopharmaceutical Research* **2** (2), 292–299. doi:10.1198/sbr.2009.0074.

Zhang, D., Han, D. M. & Song, X. F. 2020 Impacts of the Sanmenxia Dam on the interaction between surface water and groundwater in the Lower Weihe River of Yellow River Watershed. *Water* **12** (6), 1671–1688. doi:10.3390/w12061671.

Zhang, K. L., Feng, R. R., Zhang, Z. C., Deng, C., Zhang, H. J. & Liu, K. 2022a Exploring the driving factors of remote sensing ecological index changes from the perspective of geospatial differentiation: a case study of the Weihe River Basin, China. *International Journal of Environmental Research and Public Health* **19** (17), 10930–10956. doi:10.3390/ijerph191710930.

Zhang, Y. W., Zhang, B., Ma, B., Yao, R. P. & Wang, L. B. 2022b Evaluation of the water conservation capacity of the Weihe River Basin based on the integrated valuation of ecosystem services and tradeoffs model. *Ecohydrology* **15** (8), 2465–2475. doi:10.1002/eco.2465.

Zhao, P. P., Lu, H. S., Fu, G. B., Zhu, Y. H., Su, J. B. & Wang, J. Q. 2017 Uncertainty of hydrological drought characteristics with copula functions and probability distributions: a case study of Weihe River, China. *Water* **9** (5), 334–348. doi:10.3390/w9050334.

Zhao, Z., Li, A. L., Ma, Y. M., Lian, H. D. & Zhang, L. 2019 Analysis of remote sensing technology applied on hydrology and water resources-taking Weihe's ecology as an example. *Applied Ecology And Environmental Research* **17** (5), 11887–11899. doi:10.15666/aeer/1705_1188711899.

First received 24 February 2023; accepted in revised form 18 June 2023. Available online 30 June 2023